Physics – Uspekhi **51** (9) 955 – 974 (2008)

CONFERENCES AND SYMPOSIA

PACS numbers: 01.10.Fv; 61.80.Jh, 64.70.Kb, 81.40.Wx;
05.10.Ln, **64.60. – i**, **75.40. – s**; **42.55. – f**, 42.60.By, **42.65. – k**

Equilibrium and highly nonequilibrium states of condensed matter (Scientific session of the Physical Sciences Division of the Russian Academy of Sciences, 21 April 2008)

V V Ovchinnikov; A K Murtazaev; E A Khazanov, A M Sergeev

DOI: 10.1070/PU2008v051n09ABEH006795

On 21 April 2008, a scientific session of the Physical Sciences Division of the Russian Academy of Sciences was held at the conference room of the Lebedev Physical Institute, RAS. The following talks were presented:

(1) **Ovchinnikov V V** (Institute of Electrophysics, RAS (UB), Ekaterinburg) "Radiation-dynamic effects. Potential for producing condensed media with unique properties and structural states";

(2) **Garnov S V** (Prokhorov General Physics Institute, RAS, Moscow) "Femtosecond laser plasma of multiply ionized gases";

(3) **Murtazaev A K** (Institute of Physics, Dagestan Scientific Center, RAS, Dagestan State University, Makhachkala) "Critical properties of frustrated spin systems on a stacked triangular lattice";

(4) **Khazanov E A, Sergeev A M** (Institute of Applied Physics, RAS, Nizhnii Novgorod) "Petawatt lasers based on optical parametric amplifiers: their state and prospects".

Summaries of talks 1, 3, and 4 are given below.

PACS numbers: 61.80.Jh, 64.70.Kb, 81.40.Wx
DOI: 10.1070/PU2008v051n09ABEH006609

Radiation-dynamic effects. Potential for producing condensed media with unique properties and structural states

V V Ovchinnikov

1. Introduction

For some aspects of solid state radiation physics — the 'low-dose effect' (the influence of ionizing radiation on the structure and properties of materials at an insignificant number of displacements per atom [1, 2]) and 'long-range effects'[1] arising during the irradiation of condensed media by heavy charged particle beams [3, 4] — classical models fail to provide convincing explanations. Nor, as is quite obvious, are generation processes due to the irradiation of Frenkel pairs, dislocations, and other defects of any help if taken alone because the long-range scales involved are often many times larger than the size of polycrystalline grains (whose boundaries serve as sinks or barriers for structural defects). The overwhelming majority of proposed long-range mechanisms neglect the response of the irradiated medium, even though this response can be of crucial importance in some cases.

In this talk, various aspects of the effect of ionizing radiation on a substance are briefly analyzed in relation to the above problems. It is argued that the *radiation-dynamic* (RD) effect of ionizing radiation on *metastable* media is of particular importance.

In real life, the distribution of defects that form in a material irradiated with particles heavier than electrons — such as reactor neutrons, fission fragments, and accelerated ions (with energies from $10^3 - 10^4$ eV to $10^7 - 10^8$ eV) — cannot be represented as a system of single Frenkel pairs uniformly distributed over the volume of the material (Fig. 1a), but is qualitatively different from this [5, 6] (Fig. 1b – d, 2a).

The primary atoms that neutrons knock out of lattice sites displace other atoms, and so on, thus producing one or more dense cascades[2] of atomic displacements (Fig. 1b). Each such cascade contains from hundreds to tens of thousands of the target material atoms, many of which (from several hundred to several tens of thousands) are knocked out of their lattice positions. As a cascade develops, all the atoms, including those not displaced from lattice sites, change their kinetic energy many times in collisions with neighboring atoms, until the so-called thermal spike forms (see Section 2.1).

Interactions involving nuclear excitations and reactions are relatively few and of little or no importance for the analysis that follows.

The stopping of fission fragments, accelerated ions, and fast recoil atoms in condensed matter is due not only to elastic collisions with the atoms of the target but also to some energy being inelastically transferred to the electron system for the excitation and ionization of atoms (inelastic losses).

As the fission fragments and high-energy ions are stopped, the share of inelastic losses decreases, with the result that the particles increasingly produce primary recoil atoms (typically with energies in the range $10^4 - 10^6$ keV). Each of these gives rise to one or more dense atomic

[1] Ion bombardment experiments have shown that changes in the material structure and properties occur at a depth several orders of magnitude grater than the projected ion range.

[2] The term 'dense' refers to a cascade that has no branches in it, such that all the atoms in a compact region participate in collisions.

Uspekhi Fizicheskikh Nauk **178** (9) 991 – 1011 (2008)
DOI: 10.3367/UFNr.0178.200809e.0991
Translated by E G Strel'chenko, E Yankovsky, and N A Raspopov; edited by A M Semikhatov

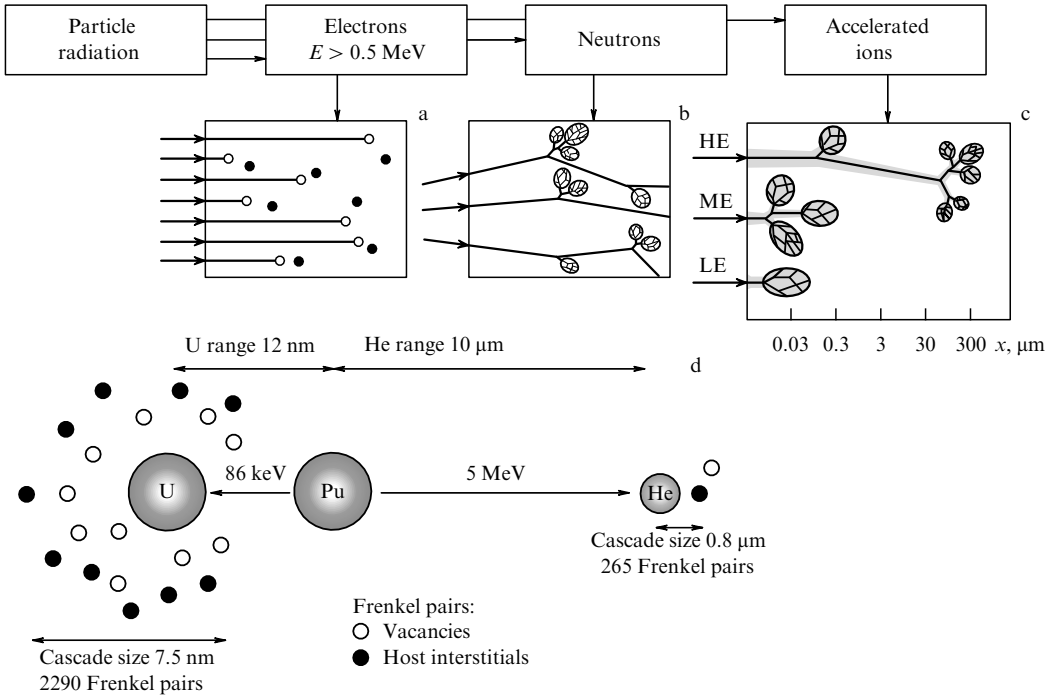

Figure 1. Damage types due to particle radiation: (a) electrons (single Frenkel pairs); (b) neutrons (passage zones for dense cascades of atomic displacements (i.e., depleted zones) are shown in Fig. 2a, e – h); (c) heavy ions and fission fragments (ionization and dense cascade regions); (d) dense cascade formation by a fission fragment in plutonium [7]. Panel c is a schematic not-to-scale diagram of high-energy (HE), medium-energy (ME), and low-energy (LE) ion radiation scenarios (a conventional classification is given in Ref. [8]).

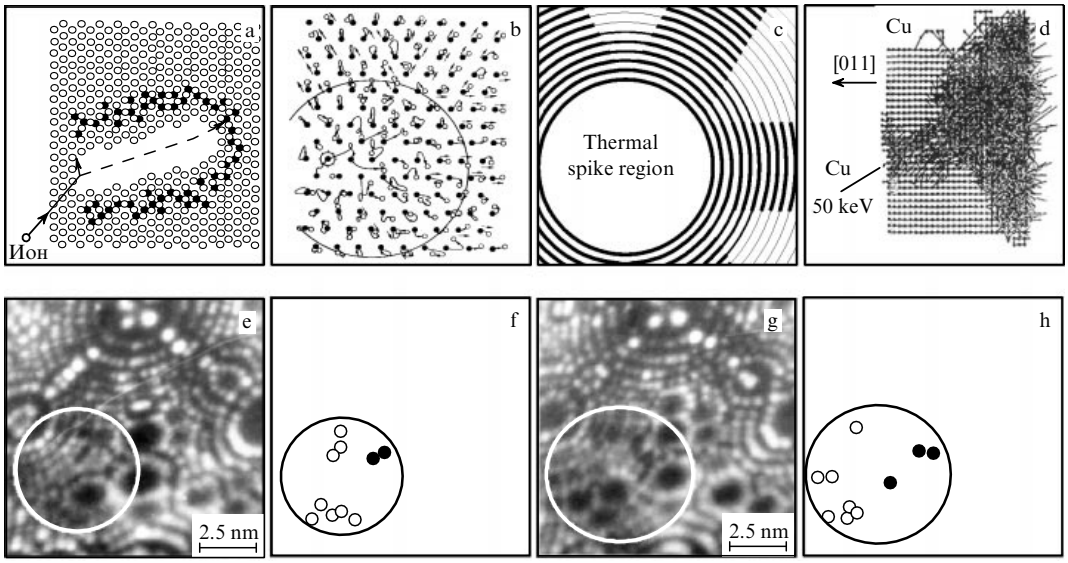

Figure 2. Structure and dynamics of radiation damage regions. (a) Schematic of the depleted zone emerging after the passage of an atomic displacement cascade [12]. (b) Results of a molecular dynamic modeling of a thermal spike [13]. (c) Schematic of how the focusing mechanism forms plane wave segments from the original spherical wave (see, e.g., Ref. [14]). (d) Development of a dense cascade: Cu → Cu (supercomputer modeling [15]). (e, g) Atomic resolution field-ion images of depleted zones in pure platinum irradiated by reactor neutrons with $E > 0.1$ MeV (the flux density 3.5×10^{22} cm^{-2}) [16]; the images in panels e and g are separated by two atomic layers (the atomic layers were removed one by one with an electric field). (f, h) The corresponding vacancy (white dots) and interstitial (black dots) distribution schematics.

displacement cascades, the same as with irradiation by reactor neutrons (Fig. 1c).

For low and medium-energy (1 – 100 keV [8]) ions, elastic and inelastic energy losses are comparable in value and mainly occur in the region of dense atomic displacement cascades. The reader is referred to Refs [8, 9] for estimates of the proportion of elastic and inelastic losses in a dense cascade. Other possible stopping mechanisms contribute negligibly at energies of interest here.

2. Radiation-dynamic effects due to particle irradiation

2.1 Post-cascade shock wave formation during the evolution of dense atomic collision cascades

As a cascade of atomic collisions develops, it takes about 10^{-12} s to 'thermalize,' i.e., to enter the 'thermal spike' state, in which the velocity distribution of the particles becomes Maxwellian [10]. (For comparison, the time scales of a chemical and a nuclear explosion are 10^{-5} and 10^{-8} s, respectively).

For a monoenergetic beam of heavy ions, the cascade region typically has the shape of an ellipsoid of rotation, if there are no channeling effects and the beam is normal to the surface of a flat target [9, 11] (Fig. 3a). Estimates for ions that are not very light are conveniently obtained by using the effective cascade radius R_0, which is taken to be equal to $\Delta R_\perp$, $\Delta R_\parallel$, or $(\Delta R_\parallel \Delta R_\perp^2)^{1/3}$ depending on the situation. For a dense cascade produced by an ion or a recoil atom with the energy $E > 10$ keV, the typical R_0 value is ~ 5 nm.

Favorably, even for metals, the time needed to remove heat from a region this size is sufficiently large, no less than 10^{-11} s according to Ref. [10], which exceeds the cascade thermalization time by at least an order of magnitude.

The maximum temperature of the cascade region can be estimated as the ratio of the energy E of a primary recoil atom (or an accelerated ion) to the number of atoms of the substance in the thermalized cascade.[3] This estimate agrees quite well with Monte Carlo simulations [10, 11] and experimental data [18, p. 90; 19]. For heavy ions, the maximum temperature of the cascade region can exceed 5000 – 6000 K. It is noteworthy that this temperature increases as the energy of the primary atom (or accelerated ion) decreases. The decisive factor here is how the volume of the cascade depends on energy (as the data in Ref. [19] confirm). Also, the cascade region can only be in a quasi-equilibrium state, which becomes increasingly nonequilibrium as the energy of the knocked out primary atom decreases and the cascade size decreases.

The energy release rate in dense cascades is nearly the same as in a nuclear explosion (with a nuclear plasma at $\sim 10^8$ K), although the specific energy release is more than 10^4 times lower.

The pressure limit in a cascade region, which can be estimated as $p = (E/V)(c_P/c_V - 1)$ [20, 21], is at least several tens of kilobars. When abruptly expanded, a strongly heated cascade region can produce a shock wave of a nearly spherical shape if the ions are not too light (Fig. 2b, 3a, b). Due to the operation of mechanisms that focus the wave energy into selected crystal directions [13 – 15], the transformation of the spherical wave into plane wave fragments is possible (Fig. 2b – d).

The primary recoil atoms for the reactor ion subsystem and heavy charged particles are most likely in the energy range between tens and hundreds of kiloelectronvolts and produce one or more dense atomic collision cascades over the length of their range ($\lesssim 1$ μm). Thus, the emergence of nanosize regions of explosive energy release with the emission of shock waves is common for various types of particle irradiation (except for particles less massive than nucleons).

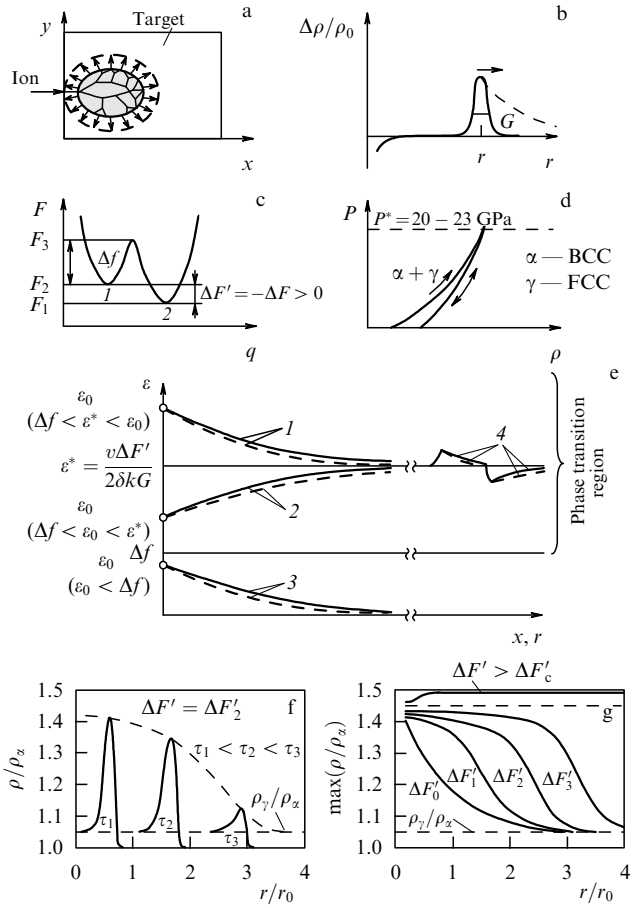

Figure 3. Schematic nature of radiation-dynamic structure – phase transformations. (a) Formation of a nanoshock wave at the final evolution stage of a dense atomic displacement cascade. (b) Profile of the post-cascade shock wave (relative change in the density of the medium) [22]. (c) Schematic change in the free energy of the system (*1*, metastable state; *2*, stable state). (d) Irreversible phase transition in the hydrostatically loaded $Fe_{69}Ni_{31}$ alloy. (e) The solution of the equation $d\varepsilon/d\xi = -2\beta\varepsilon + \Delta F'/(kG)$ for a plane wave (solid lines) and a spherical wave (dashed lines); lines *1*, *2* and *4* are an undamped, self-amplitude-modulated wave, *3* is a damped wave. (f, g) Numerical solutions of hydrodynamic equations; (e) the wave profile as a function of time; (g) atomic density change at the wave peak for different values of $\Delta F'_i$ ($\Delta F'_0 < \Delta F'_1 < \Delta F'_2 < \Delta F'_3$), an undamped phase-transition wave at $\Delta F' > \Delta F'_c$. BCC and FCC stand for bulk centered cubic and face centered cubic.

The same is true for the self-irradiation of fissioning materials (Fig. 1d), which is a process involving the aging of materials [7].

We note that until recently, the explosive energy release by emitting solitary shock waves has not been considered in studying the behavior of condensed matter, including media with high stored energy under irradiation conditions.

2.2 Propagation of post-cascade shock waves in stable media

The propagation of post-cascade shock waves in thermodynamically equilibrium (*stable*) media has been the subject of many studies, in particular, Refs [22 – 24]. According to some estimates (see Refs [22, 25]), the pressure at the front of a

[3] Strictly speaking, this is true only for dielectrics. In semiconductors and metals with few structural defects and a large electron mean free path, the energy (about $0.2E$ according to Ref. [8]) released in dense cascades into the electron subsystem (electron slowdown) is carried away from the dense cascade region [17] through the electron subsystem so fast that it has no time to be 'pumped' into the energy of neutrons.

post-cascade shock wave in the case of irradiation with heavy ions can exceed the yield strength limit of solids, not only the real (due to stresses of unblocked dislocations) but also the theoretical one. In the latter case, stresses at the front of a shock wave are sufficient for a defectless material to start to flow with mixing of atoms, giving rise to new dislocations and other defects behind the wave front. Following the region of increased pressure is an unloading wave [22].

The anomalous mass transfer [26] due to a large number of solitary shock waves can be an alternative to diffusive mass transfer. This process sharply increases the number of displacements per atom in the bulk of the material (see, e.g., Ref. [27]), although the temperature can be insufficient for the normal and radiation-enhanced diffusion to occur. The difference in pair-interaction energies w_{ij} for different atomic species under the conditions of a 'radiation-dynamic' material flow at the wave front can lead to a correlated rearrangement of atoms [21] and, ultimately, to the occurrence in a condensed medium of intraphase rearrangements and phase transformations [21, 27] that produce the short- and long-range atomic order normally controlled by diffusion processes.

As shown in Ref. [28], a shock wave can overcome the boundary of a grain, losing about 10 – 20% of its energy in the process.

Due to their high front pressures, post-cascade shock waves can also initiate diffusionless processes of the martensitic transformation type (some features of a diffusionless transformation initiated by ion irradiation can be seen in the inverse $\alpha \to \gamma$ transformation in the $Fe_{69}Ni_{31}$ alloy [29]; see also Section 4.1, Fig. 5a).

It is readily calculated that for $R_0 \sim 5-10$ nm, a spherical post-cascade wave in a stable medium travels at best several tens of nanometers before being damped tenfold, making it impossible to explain 'long-range effects' at distances of tens, hundreds, or even thousands of micrometers (see Section 4).

2.3 Theoretical model of self-sustained (self-propagating) radiation-induced structure – phase transformations in metastable media

The author and his colleagues studied [29, 30] post-cascade wave propagation in metastable media, that is, media that are not at the absolute (global) minimum of energy but at a certain intermediate, shallower local minimum separated from the former by an energy barrier Δf (Fig. 3c).

To overcome the energy barrier Δf requires either an energy fluctuation (after which, in a metastable medium, the process develops spontaneously with an energy release) or a sufficient external energy supply to a certain critical volume of the material (for example, following the radiation-induced formation of a thermal spike). The irradiation, ultimately leading to the emission of shock waves, serves as a triggering mechanism here.

Overcoming the potential barrier involves an energy release that exceeds Δf by the amount $\Delta F' = -\Delta F > 0$ (Fig. 3c). If the energy dissipation rate (i.e., the damping rate) of a wave propagating in a metastable medium does not exceed the energy release rate at the phase transformation front, then this wave is expected to become self-propagating.

In Ref. [29], the propagation of a hard-profile soliton wave in a metastable medium (Fig. 3b) is considered by replacing the usual damping equation $d\varepsilon/d\xi = -2\beta\varepsilon$ by the equation $d\varepsilon/d\xi = -2\beta\varepsilon + \Delta F'/(kG)$, which accounts for the energy release at the wave front driving the structure – phase transformation and in which ε is the energy at the wave profile maximum (per atom/molecule of the medium), $\xi = x$, $\beta = \delta/v$ for a plane wave and $\xi = r$, $\beta = \delta/v + 1/r$ for a spherical wave (x and r are the front coordinates, δ is the damping coefficient, and v is the wave velocity), and k and G are the shape factor and the half-height width of the wave profile (Fig. 3b) (for a Gaussian wave profile, $k = \sqrt{\pi/4\ln 2} \approx 1.06$ [29]). For a plane wave, the solution is given by

$$\varepsilon(x) = \begin{cases} \varepsilon_0 \exp\left[-\dfrac{2\delta(x-x_0)}{v}\right], & \varepsilon_0 < \Delta f, \\ \varepsilon^* - (\varepsilon^* - \varepsilon_0)\exp\left[-\dfrac{2\delta(x-x_0)}{v}\right], & \varepsilon_0 \geqslant \Delta f, \end{cases} \tag{1}$$

where $\varepsilon^* = \Delta F'/(2\delta kG)$.[4]

For $\varepsilon_0 < \Delta f$ (Fig. 3e), a usual damped wave is observed. The simultaneous conditions $\varepsilon_0 > \Delta f$ and $\varepsilon^* > \Delta f$ produce an amplitude-self-regulated wave (a wave that restores its amplitude when perturbed by medium inhomogeneities). For other relations between the control parameters ε_0, Δf, and ε^*, the solutions are also rather simple to analyze. Using the damping rate estimate obtained above for a spherical post-cascade wave in a stable medium (the corresponding range radius ~ 100 nm) and noting that the half-height profile width of a solitary wave is of the order of 1 nm according to Ref. [22], we easily estimate that the condition $\varepsilon^* > \Delta f$ is already satisfied at about $\Delta F'_{cr} > 0.02\Delta f$.

This means that a wave becomes undamped even if it is fed very little in the course of structure – phase transitions. It is only necessary that the energy of an accelerated particle that is released in the cascade region (per cascade atom: $E/N \geqslant \varepsilon_0$) be confidently larger than the energy required to do the work of overcoming the energy barrier Δf between the stable and metastable states, and that the characteristic size (radius) R_0 of the cascade significantly exceed the characteristic heat conduction length (to not give heat enough time to 'run away' from the cascade region before the cascade thermalizes and emits a shock wave):

$$\sqrt{\varkappa\tau} \ll R_0 < \left[\frac{E}{(4/3)\pi\rho\Delta f}\right]^{1/3}, \tag{2}$$

where τ is the cascade thermalization time, $\varkappa$ is the thermal diffusivity, and ρ is the atomic density of the material [cm^{-3}].

In Ref. [30], we treated this problem with a more rigorous hydrodynamic method based on the use of the Altshuler – Bushman – Fortov equation of state

$$\frac{\partial\rho}{\partial\tau} + \frac{\partial(\rho u)}{\partial r} + \frac{2}{r}\rho u = 0, \tag{3}$$

$$\frac{\partial u}{\partial\tau} + u\frac{\partial u}{\partial r} + \frac{1}{\rho}\frac{\partial p}{\partial r} = 0, \tag{4}$$

$$\frac{\partial\varepsilon}{\partial\tau} - \frac{p}{\rho^2}\frac{\partial p}{\partial\tau} = 0, \tag{5}$$

$$-\rho_\alpha c = \rho(u-c), \tag{6}$$

$$\rho_\alpha c^2 + p_0 = \rho(u-c)^2 + p + p_0, \tag{7}$$

$$\frac{1}{2}c^2 + \frac{\gamma_\alpha}{\gamma_\alpha - 1}\frac{p_0}{\rho_\alpha} + \Delta F' = \frac{1}{2}(u-c)^2 + \frac{\gamma_\gamma}{\gamma_\gamma - 1}\frac{p+p_0}{\rho} + \frac{\gamma_\gamma - 5/3}{2(\gamma_\gamma - 1)}\frac{p + p_0 - p_0(\rho/\rho_\gamma)^{\gamma_\gamma}}{\rho\Gamma_\gamma}, \quad \gamma_s = 2\Gamma_s + \frac{1}{3} \tag{8}$$

[4] The solution for a spherical wave is more complex but qualitatively similar.

(for notation, the reader is referred to Ref. [23], in which another version of the equation is given). Specifically, the problem was concerned with the alloy $Fe_{69}Ni_{31}$, in which we had previously observed [31–35] an inverse BCC (α) $\rightarrow$ FCC (γ) phase transformation initiated by 20 keV Ar^+ irradiation and terminating in several seconds of irradiation at a temperature lower than that for a similar thermal transformation (see Section 4.1, Fig. 5a).

It is known [36] that applying static pressure of the order of 20 GPa causes an irreversible BCC (α) $\rightarrow$ FCC (γ) transformation (Fig. 3d).

Importantly, the hydrodynamic equations were written by noting that the material properties experience a sudden jump at the transition from the BCC (α) to the FCC (γ) state:

$$\varepsilon = \varepsilon_s = \varepsilon^{B_0^s}_{\Gamma_s}(p,\rho)\,,$$

$$\varepsilon = \begin{cases} \varepsilon_\alpha = \varepsilon^{B_0^\alpha}_{\Gamma_\alpha}(p,\rho)\,, & \rho_0 = \rho_0^\alpha\,,\ B_0 = B_0^\alpha\,,\ \Gamma = \Gamma_\alpha \\ & \text{for } \alpha \text{ phase}\,, \\ \varepsilon_\gamma = \varepsilon^{B_0^\gamma}_{\Gamma_\gamma}(p,\rho)\,, & \rho_0 = \rho_0^\gamma\,,\ B_0 = B_0^\gamma\,,\ \Gamma = \Gamma_\gamma \\ & \text{for } \gamma \text{ phase} \end{cases},$$

$$\varepsilon = \frac{1}{\Gamma\rho}\left\{p - \frac{B_0}{2\Gamma+1/3}\left[\frac{\Gamma-2/3}{2\Gamma-2/3}\left(\frac{\rho}{\rho_0}\right)^{2\Gamma+1/3} - (\Gamma+1)\right]\right\}, \tag{10}$$

$$\varepsilon_\alpha = \varepsilon_\gamma + \Delta F'\,, \tag{11}$$

$$p = p_s = p^{B_0^s}_{\Gamma_s}(\rho)\,,$$

$$p = \begin{cases} p_\alpha = p^{B_0^\alpha}_{\Gamma_\alpha}(\rho) & \text{for } \alpha \text{ phase}\,, \\ p_\gamma = p^{B_0^\gamma}_{\Gamma_\gamma}(\rho) & \text{for } \gamma \text{ phase}\,, \end{cases} \tag{12}$$

$$p = \frac{B_0}{2\Gamma+1/3}\left[\left(\frac{\rho}{\rho_0}\right)^{2\Gamma+1/3} - 1\right], \tag{13}$$

where B_0 is the zero-temperature hydrostatic compression modulus, Γ is the Grueneisen constant, ρ is the atomic density, and $s = \alpha, \gamma$. The wave damping effect was taken into account by introducing the pseudoviscosity of the medium in accordance with the Neumann–Richtmyer equation [30].

The numerical solution of the above equations shows (see Fig. 3f, g) that as more energy is released at the wave front in the course of the phase transformation, a plateau develops and steadily expands on the wave-amplitude-versus-distance plot, and a regime where the transformation wave becomes undamped is entered for $\Delta F' > \Delta F'_c$. This, by and large, confirms the modeling results mentioned above concerning a hard-profile soliton wave propagating in a metastable medium.

3. Various types of radiation-dynamic transformations

Because of the extremely low diffusion rate of atoms at $T < T_c$, where T_c is a kind of threshold for 'defreezing' diffusion processes, some alloys can exhibit a hysteresis for direct and reverse structure–phase transitions (due to finite-rate heating and cooling, respectively) and allow a high-temperature state to be retained at lower temperatures by means of a fast quenching. At any temperature $T < T_c$, the alloy can be in either of two states, stable or metastable, depending on its past history.

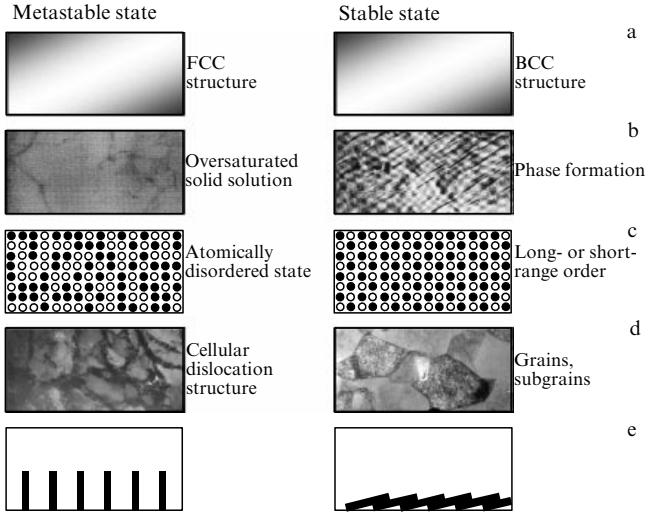

Figure 4. Examples of stable and unstable states at room temperature. (a) $Fe_{69}Ni_{31}$ alloy experiencing a BCC $\leftrightarrow$ FCC phase transformations ($\alpha \leftrightarrow \gamma$) on heating and cooling. (b) Oversaturated solid solutions Al–4% Cu (with heating-induced formation of Guinier–Preston zones, θ' and θ phases [37], and Fe–8% Mn (with formation of a γ phase) [38]. (c) Self-ordering alloys with a long-range (Fe–Al, Pd–Cu, Fe–Pd–Au) [27, 29, 32, 33, 39–41] and short-range (Fe–Cr, Fe–Si) [21, 42] atomic order. (d) Hardened and annealed industrial aluminum alloys [43–46] (the alloys shown are those in which, along with thermal annealing, the author and his colleagues observed *fast radiation annealing* at lowered temperatures). (e) Domino effect.

In Figs 4a–d, the stable and metastable states of metal alloys at room temperature are illustrated for alloys in which, in addition to thermal annealing, fast radiation annealing was observed by the author and coworkers at a lowered temperature (Fig. 4d).

If a system of N domino pieces (Fig. 4e) structured in a certain way is taken (as it can be) as a model for a metastable medium, then heating the medium into a stable state can be likened to simultaneously toppling N pieces and imparting N energy units to them (which corresponds to imparting energy to the entire volume of the substance). The triggering of a self-propagating process through the toppling of a single domino piece by imparting a single energy unit to it is analogous to a radiation-dynamic transformation.

4. Material treatment using radiation-induced effects

In all the experiments described below, we chose metastable media with increased stored energy as the objects affected by the action of accelerated ion beams (N^+, Ar^+, Fe^+, Cu^+).

In each experiment, the irradiation temperature was monitored and the observed effects were compared with those produced by a purely thermal influence (in the absence of irradiation) when the ion beam heating regime is exactly reproduced. In some cases, up to 100% of the ion beam power density was steadily replaced by light radiation such that the stationary temperature of the irradiation (and hence the intensity of thermostimulated processes) remained unchanged. The irradiation temperatures that were typically used were extremely low, much below the threshold for 'defreezing' diffusion (above the threshold, thermostimulated diffusive phase transformations occurring in very short times are already possible).

4.1 Modifying the resistive properties of alloys

In Figs 5a – b, results of the effect of accelerated ion beams on the resistive properties of the alloy systems Fe – Ni [29], Fe – Pd – Au [27, 29, 41], and Pd – Cu [39, 40] are presented and compared with those from a usual thermal treatment.

All three alloy systems share the feature that because of an RD component[5] in the particle (corpuscular) irradiation effect on a substance, the *metastable-to-stable* transition (see the caption to Figs 5a – c) has a much lower temperature threshold (by 50 to 165 K, depending on the alloy) compared to the thermostimulated transition.

For high-resistance $FePd_2Au$, a virtually zero temperature coefficient of electric resistivity (TCR) was achieved (Fig. 5b) due to a special type of a long-range order forming in the bulk of the material under the irradiation conditions [27, 41].

The reasons expounded in Section 2.2 underlie a sharp increase in the low-temperature mobility of atoms in the bulk of disordered alloys $FePd_2Au$ and $Pd_{45}Cu_{55}$ (in samples 100 μm thick studied) under their surface[6] irradiation by Ar^+ and Cu^+ ions (Fig. 5b, c) and, accordingly, a decrease in their ordering temperature when heated by an ion beam. This is confirmed by a detailed X-ray diffraction analysis [27, 39, 40].

The change in the electric resistance and TCR of the $Fe_{69}Ni_{31}$ alloy (Fig. 5a) can also occur because a short-range order forms on it at anomalously low temperatures.

That a phase transition is complete to a degree depending on the radiation dose can be due to the focusing effect of the vibration energy of the lattice [14], resulting in the initially spherical post-cascade wave transforming into plane-wave fragments (Fig. 2b – d). Another possible reason is that each separate post-cascade wave increases the degree of transformation only partially when it passes [27, 29].

4.2 Changing the magnetic properties of alloys

A major discovery is that radiation treatment strongly affects the magnetic properties of $Fe_{69}Ni_{31}$ [29, 32 – 34] and the atomic [42] and magnetic [47 – 49] structure and electrical engineering properties of transformer steels, permalloy, and amorphous and nanocrystalline magnetically soft materials (finemets).

The effect of the heating of a material concomitant to its irradiation by high-intensity ion beams was eliminated by using an intermittent or a low-frequency pulse-repetitive irradiation regime.

It was demonstrated in [32 – 34] that irradiation by N^+ and Ar^+ ions in a continuous or pulse-repetitive regime significantly affects (in a regime-dependent way) the superfine magnetic structure of the Mössbauer spectrum of the $Fe_{69}Ni_{31}$ alloy, presumably because ion irradiation accelerates atomic rearrangement processes and produces a short-range order within foils 30 μm thick. The foil temperature did not exceed 200 °C. Earlier, it was only at superhigh pressures that atomic nuclei showed a similar change in superfine magnetic fields in this alloy. The spectrum does not change shape if the material is heated in the usual way to the temperature 200 °C.

In Ref. [47], the damaging (formation of defects in a surface layer tens of nanometers thick) and the radiation-dynamic effects of accelerated ions were taken into consideration to optimize irradiation regimes for the formation in anisotropic transformer steel 3424 (Fe – 3% Si) of a special *atomic* structure [42], *defect* structure, and *magnetic domain* structure much finer than the original ones shown in Fig. 5d. With this radiation treatment, losses due to magnetization reversal in the working frequency range (400 – 5000 Hz) were reduced by 6% to 20% at the induction 1.5 T. The magnetic domain structure changes to a depth of 5 to 10 μm, several orders of magnitude larger than the projected range of accelerated Ar^+ ions.

The anisotropic steel improves its electrical engineering properties because of a complex combination of factors, such as an increase in the perfection of the alloy atomic structure due to the radiation-annealing-induced ordering [47] and the formation of a unique, multilayer magnetic domain structure consisting of narrow domains (Fig. 3d) perpendicular to the easy magnetization axis [001].

A detailed study [47, 48] of how amorphous ribbons of the $Fe_{73.5}Cu_1Nb_3Si_{13.5}B_9$ alloy change their electrical engineering properties when irradiated by beams of accelerated Ar^+ ions after first being subjected to standard finishing treatment (0.5 h annealing at 530 °C to provide a nanocrystalline structure and the best ribbon properties) enable an additional (on average) 10% reduction in remagnetization losses in the frequency range from 50 Hz to 10,000 Hz due to a more perfect structure obtained.

Importantly, a patent on the combined ion-beam/thermomagnetic treatment of permalloy (Fe – 70% Ni) and transformer steel (Fe – 3% Si) [50] was obtained. The radiation-dynamic influence of an accelerated ion beam prior to the thermomagnetic treatment results in the structure of these materials being deeply refined with respect to impurities and defects [49], thus improving their electrical engineering properties. The reduction in the coercitive force compared to the purely thermomagnetic treatment is 27%. An additional reduction in the loss due to magnetization reversal in transformer steel is about 15%.

4.3 Radiation annealing of industrial aluminum alloys

The Institute of Electrophysics, Ural Branch of the Russian Academy of Sciences, and the Kamensk-Uralsk Metallurgical Works (KUMW Corp. Ltd) joined the efforts in developing radiation annealing technologies in place of the furnace annealing of rolled aluminum products (a labor and energy-consuming industrial process used to remove cold work[7]) and looking for methods for improving the intermetallic composition and mechanical properties and other performance characteristics of finished products.

Detailed studies [43 – 46, 51] of the dislocation, grain, and intermetallic structure of cold-rolled aluminum products have allowed optimizing the regimes of the fast (a few seconds) radiation annealing of industrial aluminum alloys of various compositions and developing basic technologies for this process.

The practical results of the study, together with the radiation regimes, are presented in Table 1 and in Figs 5e and 5f.

In the most general and fundamental terms, these studies have shown that the radiation effects (in this case, ion

[5] In Refs [21, 38], the contribution of the RD effect was separated by replacing up to 100% of the ion beam power density by light radiation.

[6] In solids, the mean range of heavy accelerated 10 – 100 keV ions does not exceed 1 μm.

[7] 'Cold work' refers to an increase in internal stresses and strength of a material as it undergoes cold plastic deformation. This makes the material crack-prone and its further rolling impossible without intermediate furnace annealing at increased temperatures.

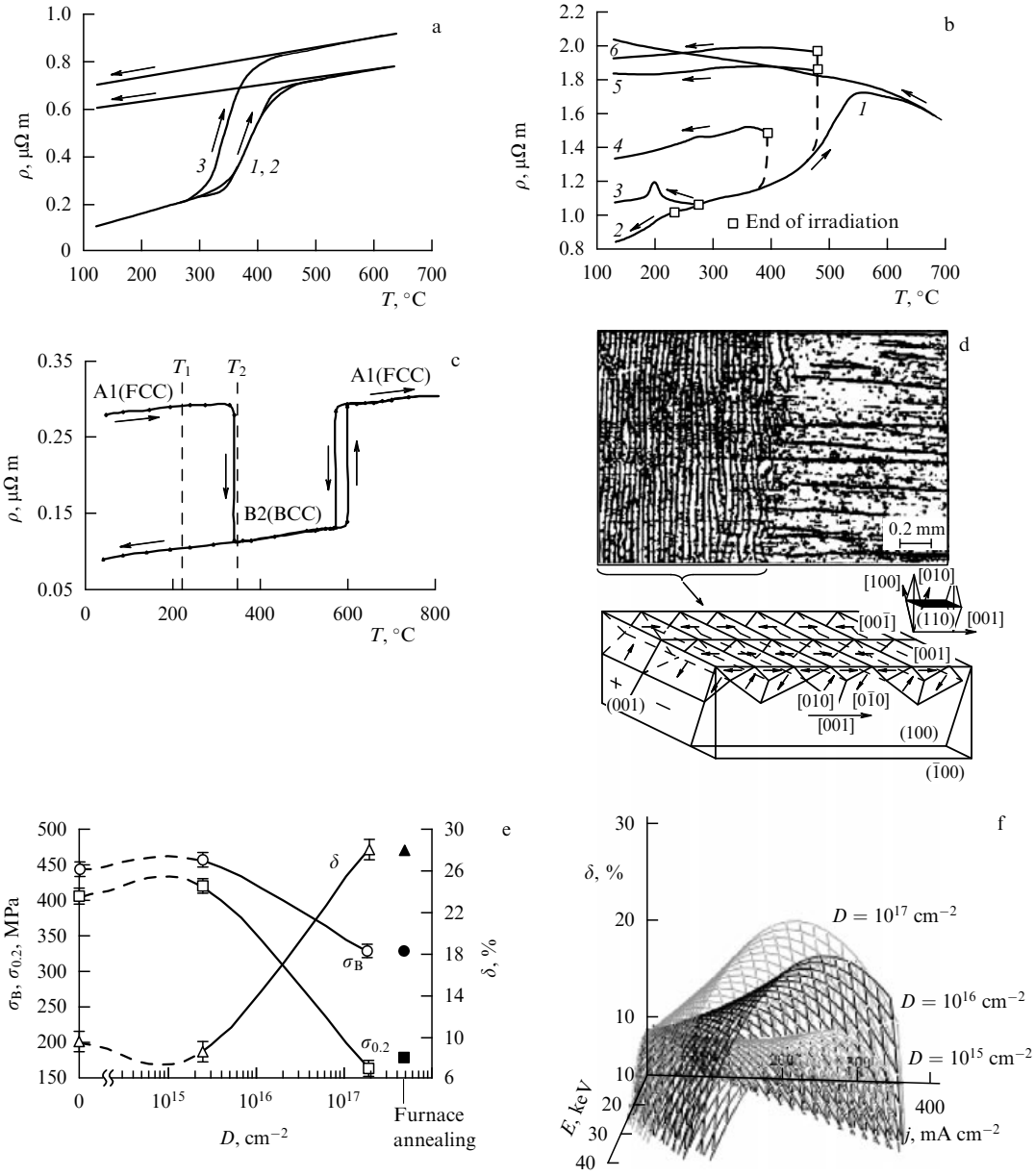

Figure 5. Examples of long-range RD effects and their radiation treatment applications. (a) Reduction in the phase transition temperature and changes in ρ and TCR for $Fe_{69}Ni_{31}$ (line *3*) irradiated by Ar^+ ions ($E = 20$ keV, $j = 80$ μA cm^{-2}) compared to the same for usual heating (lines *1*, *2*) [29]. (b) *In situ* electric resistance of the $FePd_2Au$ alloy disordered by quenching under heating and cooling (line *1*) and under irradiation (lines *2*–*6*) by Ar^+ ions ($E = 20$ keV, $j = 80$–100 μA cm^{-2}); the required irradiation temperatures were provided by using a heater and varying the ion current density. (c) Temperature of the A1 → B2 phase transition in the disordered $Pd_{45}Cu_{55}$ alloy under usual heating at 2 K min^{-1} (T_2) and under irradiation by Ar^+ ions (T_1) ($\Delta T = T_2 - T_1 = 135$ °C) [39]. (d) The magnetic domain structure and domain closure pattern in silicon iron Fe–3% Si upon irradiation by Ar^+ ions [40] (the right-hand part of the surface was masked from the irradiation; the arrows indicate domain magnetization directions). (e) Radiation and furnace annealing results for industrial alloy AMg6 (see Table 1) [43]. (f) Plasticity of the AMg6 alloy for various radiation annealing regimes.

Table 1. Mechanical properties of industrial sheets of AMg6, 1441, and BD1 aluminum alloys following thermal and radiation annealing.

Treatment	Alloy								
	AMg6			1441			BD1		
	σ_B, MPa	$\sigma_{0.2}$, MPa	δ, %	σ_B, MPa	$\sigma_{0.2}$, MPa	δ, %	σ_B, MPa	$\sigma_{0.2}$, MPa	δ, %
Cold deformation	445	407	9	315	296	3	255	246	6
Industrial annealing (2 h)	328	178	28	245	134	20	182	86	25
Radiation annealing by Ar^+ ions (5–30 s)	335	174	26	218	130	19	200	81	23

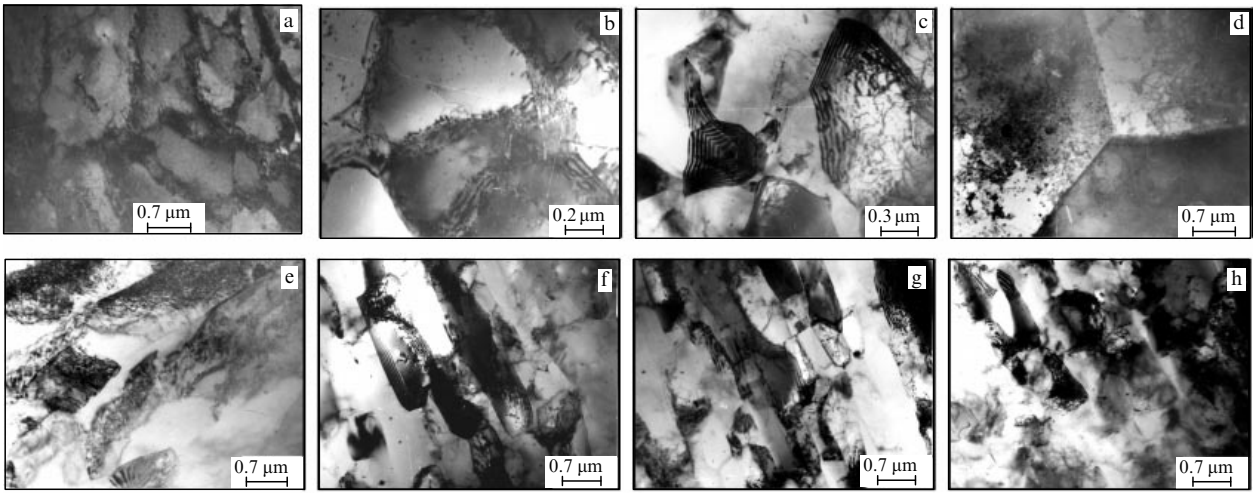

Figure 6. Changes in the BD1 alloy (Al–Cu–Mg) structure in the course of radiation annealing (a–h). (a–d) *Rolling-plane microstructure* of the BD1 *alloy*: (a) Initial post-cold-rolling state, cellular dislocation structure; (b) after-furnace annealing (250 °C, 2 h), uniform subgrain structure; (c) after-irradiation by Ar^+ ions ($E = 20$ keV, $j = 150$ μA cm^{-2}, $D = 10^{15}$ cm^{-2}, exposure time 1 s), subgrain structure; (c) the same with $D = 10^{17}$ cm^{-2}, recrystallized state. (e–h) *Cross-section microstructure* of a BD1 alloy sheet: (e) in the original state; (f–h) after irradiation by an Ar^+ ion beam with $D = 10^{16}$ cm^{-2} (near the irradiated surface, in the bulk, and near the nonirradited surface, respectively).

bombardment) offers an alternative to furnace annealing, an alternative that historically has never existed in the fields of production and treatment of metals and alloys. The phenomenon of radiation annealing is due to the RD effect of particle radiation, which is described in Sections 1–3.

Radiation annealing in aluminum [43–46, 51] and other alloys [27, 29, 31–33, 39–41] requires much lower temperatures (200 K less for aluminum alloys) and takes less time and much less energy than its thermal treatment.

Among entirely new findings, it is noteworthy that accelerated ion beams extend their influence very deep (3 mm or more for aluminum alloys) into a one-side-irradiated material; this is well confirmed by metallographic and electron microscope sheet cross section studies (Fig. 6).

In a cold-rolled state, the aluminum alloy systems studied, Al–Mg [43, 51], Al–Cu–Mg–Mn [45] and Al–Li–Cu–Mg–Zr [44], exhibit a well developed cellular dislocation structure, with dense dislocation entanglements as cell boundaries.

In the course of radiation annealing, the following processes were observed in the entire bulk of alloys (in the form of 3 mm thick sheets): polygonization with the formation of subgrains (for doses of $10^{15}-10^{16}$ cm^{-2}, the corresponding irradiation time is $\sim 1-10$ s), dissolution (10^{15} cm^{-2}) and formation ($10^{16}-10^{17}$ cm^{-2}) of new phases,[8] and the recrystallization and growth of grains ($5\times10^{16}-3\times10^{17}$ cm^{-2}) (see Fig. 6). In addition, as the radiation dose increases, the crystallographic *rolling texture* is steadily removed (Fig. 7) via a process similar to but distinct from furnace annealing [46]. The fast polygonization process involving the formation of grains is presumably due to the radiation-induced explosive rearrangement of the dislocation structure [44].

Using regression analysis techniques, the strength limit σ_B, the yield strength $\sigma_{0.2}$, and the unit elongation δ were obtained as (multidimensional) functions of the radiation parameters (the energy E, the ion current density j, and the dose D) (Fig. 5f).

[8] In furnace annealing, the intermetalilic composition of aluminum alloys remains unchanged.

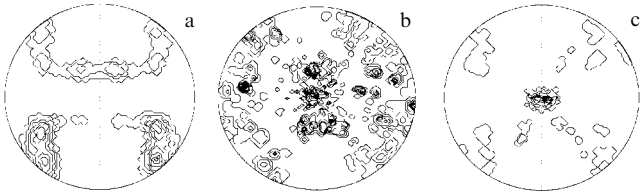

Figure 7. How the 1441 alloy (AL–Li–Cu–Mg) changes its crystallographic texture in the course of radiation annealing. (200) *pole figures*: (a) post-cold-rolling state, (b) after furnace annealing at 370 °C for 2 h, (c) after irradiation by Ar^+ ions ($D = 5.6\times10^{16}$ cm^{-2}).

To realize radiation annealing technology, special facilities and equipment have been developed (Fig. 8), including a service model of a *ribbon source* of ions with the beam cross section 20×1200 mm for the radiation annealing of sheet-rolled products [52] (Fig. 8c); a facility for the two-side treatment of moving sheets of aluminum alloys by counter beams of accelerated ions (with a special source for industrial applications [53]) (Fig. 8a, b); and a facility for the crystallization of alloys under irradiation (Fig. 8d).

5. Conclusion

To summarize, there is, in fact, no alternative to the radiation dynamic action as a way to initiate self-propagating structure–phase transformations in metastable media in order to modify their properties. Using a chemical explosion with the characteristic time $\tau = 10^{-5}$ s requires, in accordance with Eqn (2), increasing the zone of volume energy release ($d_0 = 2R_0$) to several centimeters and increasing the energy release rate to about that produced by a meteorite or a military propellant, which is clearly unacceptable given our purposes. Furthermore, other similarity aspects of influences under considerations should be given a detailed analysis.

Figure 8. Equipment for the radiation treatment of materials by ion beams. (a) Ion implanter for the bilateral treatment of moving alloy sheets by counter ion beams [52]. (b) Counter ion beams photographed through the chamber window. (c) Service model of a ribbon source of accelerated ions with the cross section 20 × 1200 mm for the treatment of sheet rolled products [53]. (d) Facility for the radiation treatment of melts.

Based on the above, the following conclusions can be drawn.

(1) Various particle radiations, except for the radiation of particles lighter than a nucleon, produce zones of explosive energy release in condensed media, emitting shock waves in the process. The energy density in such a zone can exceed 0.5 eV per atom. The energy carried away by the shock wave is sufficient to initiate a transition in metastable media into a state with a lower free energy.

(2) Even for a relatively small positive balance of the phase transition ($\Delta F' \sim (0.01-0.1)\Delta f$), the particle irradiation can initiate self-sustained (self-propagating) phase transformations at the fronts of post-cascade nanoshock waves. Such transformations explain the nature of the low-dose effect and of dynamic long-range effects observed under irradiation.

(3) Hydrodynamically described irradiation-induced shock wave processes and phase transformations, as well as structural chain-reaction-type rearrangements initiated by the propagation of waves (related to the unblocking of dislocations, annihilation of various types of defects [44], etc.), have been termed *radiation-dynamic* effects, as opposed to the well-studied radiation-stimulated migration processes.

(4) The plastic flow of material at the front of a post-cascade wave can be an alternative to diffusive mass transfer in condensed media. The mobility of atoms also increases with a decrease in the activation energy for atomic migration (all the way to making the process activationless) due to the lattice being radiationally 'shaken' by the emitted waves.

(5) Experimental data suggest that processes most affected by RD are those not requiring long-range mass transfer, such as massive (martensite) transformations, atomic disorder – order transformations, the aging of oversaturated solid solutions with the precipitation of disperse phases, and explosive dislocation rearrangements, etc.

(6) The concept of the radiation-dynamic effect of radiations on metastable media suggests the *radiation annealing* of condensed media as an alternative to furnace annealing. The efficiency of radiation annealing has been demonstrated by the improvement in the electric and magnetic properties of materials and by the increase in the plasticity of aluminum alloys (the removal of cold work). States that can be achieved with radiation annealing may differ widely from those occurring with furnace annealing, offering new possibilities for controlling the material properties. Radiation annealing

consumes much less energy, takes less time, and allows a reduction of 50 to 200 K in temperature.

References

1. Mamontov A P, Chernov I P *Effect Malykh Doz Ioniziruyushchego Izlucheniya* (Low Dose Effect of Ionizing Radiation) (Moscow: Energoatomizdat, 2001)
2. Tetel'baum D I, Kuril'chik E V, Latysheva N D *Neorg. Mater.* **35** 1 (1999) [*Inorganic Mater.* **35** 344 (1999)]
3. Guseva M I "Ionnaya implantatsiya v nepoluprvodnikovye materialy" ("Ion implantation and nonsemiconductor materials"), in *Itogi Nauki i Tekhniki* (Ser. Puchki Zaryazhennykh Chastits i Tverdoe Telo. Fizicheskie Osnovy Lazernoi i Puchkovoi Tekhnologii) (Advances in Science and Technology (Ser. Charged Particle Beams and Solid State. Physical Fundamentals of Laser and Beam Technology)) Vol. 5 (Moscow: VINITI, 1984) p. 5
4. Martynenko Yu V "Effekty dal'nodeistviya pri ionnoi implantatsii" ("Long-range effects at ion implantation"), in *Itogi Nauki i Tekhniki* (Ser. Puchki Zaryazhennykh Chastits i Tverdoe Telo) (Advances in Science and Technology (Ser. Charged Particle Beams and Solid State)) Vol. 7 (Moscow: VINITI, 1993) p. 82
5. Kirsanov V V, Suvorov A L, Trushin Yu V *Protsessy Radiatsionnogo Defektoobrazovaniya v Metallakh* (Radiation Defect Formation in Metals) (Moscow: Energoatomizdat, 1985)
6. Ibragimov Sh Sh, Kirsanov V V, Pyatiletov Yu S *Radiatsionnye Povrezhdeniya Metallov i Splavov* (Radiation Damage of Metals and Alloys) (Moscow: Energoatomizdat, 1985)
7. Wolfer W *Los Alamos Sci.* **26** 227 (2000)
8. Didenko A N et al. *Effekty Dal'nodeistviya v Ionno-Implantirovannykh Metallicheskikh Materialakh* (Long-Range Effects in Ion Implanted Metal Materials) (Exec. Ed. Yu P Kolobov) (Tomsk: Izd. NTL, 2004)
9. Ryssel H, Ruge I *Ionenimplantation* (Stuttgart: Teubner, 1978) [Translated into English: *Ion Implantation* (Chichester: Wiley, 1986); Translated into Russian (Moscow: Nauka, 1983)]
10. Thompson M W *Defects and Radiation Damage in Metals* (London: Cambridge Univ. Press, 1969) [Translated into Russian (Moscow: Mir, 1971)]
11. Biersack J P, Haggmark L G *Nucl. Instrum. Methods* **174** 257 (1980)
12. Poate J M, Foti G, Jacobson D C (Eds) *Surface Modification and Alloying by Laser, Ion, and Electron Beams* (New York: Plenum Press, 1983) [Translated into Russian (Moscow: Mashinostroenie, 1987)]
13. Chudinov V G, Cotterill R M J, Andreev V V *Phys. Status Solidi A* **122** 111 (1990)
14. Levin V M, Chernozatonskii L A, in *Fizicheskaya Entsiklopediya* (Encyclopedia of Physics) (Ed.-in-Chief A M Prokhorov) (Moscow: Sovetskaya Entsiklopediya, 1990) p. 507
15. Nordlung K et al. *Nature* **398** 49 (1999)
16. Kozlov A V et al. *Voprosy Atomnoi Nauki Tekh.* **66** (1) 47 (2006)
17. Amirkhanov I V et al. *Fiz. Elem. Chastits At. Yadra* **37** 1592 (2006) [*Phys. Part. Nucl.* **37** 837 (2006)]
18. Behrisch R et al. *Sputtering by Particle Bombardment* Vol. 3 *Characteristics of Sputtering Particles, Technical Applications* (Topics in Applied Physics, Vol. 64, Ed. R Behrisch) (Berlin: Springer-Verlag, 1991) [Translated into Russian (Moscow: Mir, 1998)]
19. Ovchinnikov V V et al., in *Trudy XV Mezhdunar. Soveshch.* "*Radiatsionnaya Fizika Tverdogo Tela*" (Proc. of the VII Intern. Symp. on Radiation Physics of Solids) (*Sevastopol', 4 – 9 July 2005*) (Ed. G G Bondarenko) (Moscow: NII PMT MGIEM (TU), 2005) p. 199
20. Didenko A N, Ligachev A E, Kurakin I B *Vozdeistvie Puchkov Zaryazhennykh Chastits na Poverkhnost' Metallov i Splavov* (Effect of Charged Particle Beams on Metal and Alloy Surfaces) (Moscow: Energoatomizdat, 1987)
21. Ovchinnikov V V et al. *Appl. Phys. A* **83** 83 (2006)
22. Zhukov V P, Boldin A A *At. Energ.* **63** 375 (1987) [*At. Energy* **63** 884 (1987)]
23. Zhukov V P, Ryabenko A V *Radiation Effects Defects Solids* **82** 85 (1984)
24. Zhukov V P, Demidov A V *At. Energ.* **59** (1) 29 (1985) [*At. Energy* **59** 568 (1985)]
25. Thompson D A *Radiation Effects Defects Solids* **56** 105 (1981)
26. Bleikher G A, Krivobokov V P, Pashchenko O V *Teplomassoperenos v Tverdom Tele pod Vozdeistviem Moshchnykh Puchkov Zaryazhennykh Chastits* (Thermal Mass Transfer in Solids under High-Power Charge Particle Beams) (Novosibirsk: Nauka, 1999)
27. Ovchinnikov V V, Chernoborodov V I, Ignatenko Yu G *Nucl. Instrum. Meth. Phys. Res. B* **103** 313 (1995)
28. Psakh'e S G et al. *Pis'ma Zh. Tekh. Fiz.* **25** (6) 7 (1999) [*Sov. Tech. Phys. Lett.* **25** 209 (1999)]
29. Ovchinnikov V V *Proc. SPIE* **2259** 605 (1994)
30. Ovchinnikov V V, Erkabaev M A, in *Trudy VII Mezhnats. Soveshch.* "*Radiatsionnaya Fizika Tverdogo Tela*" (Proc. of the VII Intern. Symp. on Radiation Physics of Solids) (*Sevastopol', 30 June – 5 July 1997*) (Ed. G G Bondarenko) (Moscow: NII PMT pri MGIEM (TU), 1997) p. 22
31. Borodin S N et al. *Pis'ma Zh. Tekh. Fiz.* **15** (17) 51 (1989)
32. Kreindel' Yu E, Ovchinnikov V V *Fiz. Khim. Obrabotki Mater.* (3) 14 (1991)
33. Kreindel Yu E, Ovchinnikov V V *Vacuum* **42** (1 – 2) 81 (1991)
34. Ovchinnikov V V et al. *Surf. Coating Technol.* **64** 1 (1994)
35. Ovchinnikov V V *Izv. Ross. Akad. Nauk Metally* (6) 104 (1996)
36. Mel'nikov L A, Sokolov B K, Stregulin A I *Fiz. Met. Metalloved.* **15** (3) 357 (1963)
37. Gushchina N et al., in *Trudy XII Mezhdunar. Konf.* "*Radiatsionnotermicheskie Effekty i Protsessy v Neorganicheskikh Materialakh*" (Proc. of the XII Intern. Conf. on Radiation Physics and Chemistry of Inorganic Materials) (Ed. A P Surzhikov) (Tomsk: Izd. Tomsk. Politekh. Univ., 2003) p. 192
38. Ovchinnikov V V et al., in *Trudy XIII Mezhdunar. Soveshch.* "*Radiatsionnaya Fizika Tverdogo Tela*" (Proc. of the XIII Intern. Symp. on Radiation Physics of Solids) (Ed. G G Bondarenko) (Moscow: NII PMT MGIEM (TU), 2003) p. 587
39. Chemerinskaya L S et al., in *Trudy XV Mezhdunar. Soveshch.* "*Radiatsionnaya Fizika Tverdogo Tela*" (Proc. of the XV Intern. Symp. on Radiation Physics of Solids) (*Sevastopol', 4 – 9 July 2005*) (Ed. G G Bondarenko) (Moscow: NII PMT MGIEM (TU), 2005) p. 461
40. Chemerinskaya L S et al., in *Trudy IV Mezhdunar. Nauch. Konf.* "*Radiatsionno-termicheskie Effekty i Protsessy v Neorganicheskikh Materialakh*" (Proc. of the IV Intern. Conf. on Radiation Physics and Chemistry of Inorganic Materials) (Ed. A P Surzhikov) (Tomsk: Izd. Tomsk. Politekh. Univ., 2004) p. 278
41. Goloborodsky B Yu, Ovchinnikov V V, Semenkin V A *Fusion Sci. Technol.* **39** 1217 (2001)
42. Borodin S N et al. *Pis'ma Zh. Tekh. Fiz.* **15** (13) 87 (1989)
43. Ovchinnikov V V et al. *Izv. Vyssh. Uchebn Zaved. Ser. Fiz.* (8, Suppl.) 350 (2006)
44. Ovchinnikov V V et al. *Izv. Vyssh. Uchebn. Zaved. Ser. Fiz.* (2) 73 (2007) [*Russ. Phys. J.* **50** 177 (2007)]
45. Ovchinnikov V V et al. *Fiz. Met. Metalloved.* **105** 404 (2008) [*Phys. Met. Metallogr.* **105** 375 (2008)]
46. Ovchinnikov V V et al., in *Trudy VII Mezhdunar. Konf.* "*Vzaimodeistvie Izluchenii s Tverdym Telom*" (Proc. of the VII Intern. Conf. "Interaction of Radiations with Solids"), *Minsk, Belarus', 26 – 28 September 2007*, p. 143
47. Sokolov B K et al. *Fiz. Met. Metalloved.* **89** (4) 32 (2000) [*Phys. Met. Metallogr.* **89** 348 (2000)]
48. Dragoshanskii Yu N, Gubernatorov V V, Sokolov B K, Ovchinnikov V V *Dokl. Ross. Akad. Nauk* **383** 761 (2002) [*Dokl. Phys.* **47** 302 (2002)]
49. Gubernatorov V V et al. *Dokl. Ross. Akad. Nauk* **410** 194 (2006) [*Dokl. Phys.* **51** 493 (2006)]
50. Gubernatorov V V et al. "Sposob termomagnitnoi obrabotki magnitomyagkikh materialov" ("Thermomagnetic treatment of magnetically soft materials"), Invention Patent No. 2321644 (03.08.2006)
51. Shkol'nikov A R et al. *Izv. Tomsk. Politekh. Univ.* **308** (7) 58 (2005)
52. Gavrilov N V et al. *J. Vac. Sci. Technol. A* **14** 1050 (1996)
53. Gavrilov N V, Emlin D R, Bureev O A *Izv. Vyssh. Uchebn. Zaved. Ser. Fiz.* (8, Suppl.) 92 (2006)